A Stochastic Cloud Field Model for Generalizing Radar Derived Cloud Structure for Solar Radiative Transfer Calculations

K. F. Evans and S. A. McFarlane
University of Colorado
Boulder, Colorado

W. J. Wiscombe
National Aeronautics and Space Administration
Goddard Space Flight Center
Greenbelt, Maryland

Introduction

The radiative effects of cloud horizontal inhomogeneity may be divided into two parts (e.g., Varnai and Davies 1999): 1) the one-dimensional heterogeneity effect of optical depth variability, and 2) the horizontal transport effect of light moving between columns. For area-averaged climate applications the independent pixel approximation (IPA) correctly addresses the first effect, but not the second. There is evidence (Cahalan et al. 1994; Barker et al. 1998) that the IPA accurately predicts domain average solar fluxes in stratocumulus and even cumulus cloud fields. However, it is well known from previous Monte Carlo simulations of finite clouds (e.g., Welch and Wielicki 1984) that for high solar elevation angles horizontal transport of solar radiation results in a lower albedo compared to plane-parallel transfer, due to leakage from cloud sides. When the sun is low in the sky, the side illumination of finite clouds results in a higher albedo than the plane-parallel result. Simulations show that these three-dimensional (3D) cloud radiative effects can be quite large (>50%) for clouds with large aspect ratios (height to width) that are optically thick. However, there remains the question of how important these 3D effects are in actual cloud fields. Is the IPA adequate to predict domain average solar fluxes and heating rates or does horizontal transport have to be included?

To address this question, we need a long-term dataset of many observed 3D cloud fields, specifically for cumulus clouds that would be expected to have finite cloud effects. Many individual fields are required so the dataset is statistically representative of a particular location and cloud class, and hence gives a reliable estimate of the actual 3D radiative effects. The Atmospheric Radiation Measurement (ARM) Program millimeter wavelength cloud radar (MMCR) dataset is a good source of long-term cloud structure information. There are difficulties, however, in retrieving cloud extinction from radar reflectivity, and in relating the MMCR time-height cross sections to 3D cloud fields. In this study, we make simple microphysical assumptions for liquid phase cumulus clouds to relate radar reflectivity to optical extinction. We make the common frozen turbulence assumption with a constant advection speed to convert the time series to along-wind structure. We concentrate here on the issue of converting

two-dimensional (2D) distance-height fields to 3D fields. A stochastic cloud field generation algorithm can do this by using statistics from 2D fields to make statistically similar 3D fields.

A 3D stochastic cloud field generation algorithm is presented. It assumes horizontal isotropy and translational invariance horizontally (but not vertically). The basis for the algorithm is decomposing the input fields in Empirical Orthogonal Functions (EOFs) (principal components). The specific questions this research addresses are:

1. Can 3D tropical cumulus cloud fields be simulated from the statistics of radar time-height cloud fields?

2. Are the 2D stochastic cloud fields equivalent to the radar-derived fields in terms of broadband solar radiative transfer?

3. Is 3D radiative transfer necessary for accurate solar fluxes, or will 2D radiative transfer on radar fields suffice?

Radar Data and Cloud Retrievals

The stochastic field generation algorithm is tested using Nauru MMCR data for boundary layer clouds. Nauru is the preferred site in order to avoid the insect contamination problem in Oklahoma and also for its high frequency of cumulus clouds with potentially significant 3D radiative transfer effects. Due to a large variable offset in the ARM regression retrieval of cloud liquid water path (often >50 g/m^2 in clear sky), a radar-only algorithm is used to retrieve optical extinction. A preliminary Active Remote Sensing Clouds (ARSCL) dataset (personal communication from Eugene Clothiaux, 1999) defines the cloud boundaries. A lognormal droplet distribution with fixed number concentration of $N = 75$ cm^{-3} and standard deviation of the log of $\sigma = 0.35$ is assumed. The droplet mode radius r_0 is then obtained directly from the radar reflectivity. The liquid water content (LWC), effective radius, and extinction (assuming geometric optics) are calculated from the three parameters of the lognormal droplet distribution at each radar range gate. Retrievals are not made if the radar reflectivity is above -5 dBZ due to likely precipitation contamination or if the lidar cloud base algorithm indicates no retrieval. Interpolation of extinction across time is performed over the retrieval gaps. The extinction fields are output as byte images with a maximum of about 64 km^{-1}. The radar data for 23 days in December 1998 were processed.

The desired cloud type is boundary layer clouds, which at Nauru means cumulus clouds. Presumably because deeper clouds are precipitating, the retrieved clouds tend to be relatively shallow. Only 28 range gates (1260-m depth) starting at 600-m altitude were required to cover nearly all the clouds. The cloud retrievals were broken into 3-hour chunks, which for the 10-second ARSCL data corresponds to 1080 pixels horizontally. The conversion from time to horizontal distance was made using an advection speed that is constant in height and time over the 3-hour period. The advection speed is obtained from the LWC weighted wind profile of the Nauru radiosonde nearest in time. The selection procedure excludes periods with mean optical depth less than 0.2, more than 20% invalid data, large retrieval gaps in clouds, no radiosonde within 6 hours, or wind speeds less than 2 m/s or greater than 20 m/s.

This selection results in only 30 3-hour periods. For these 30 fields, the cloud fraction is 35%; the mean cloud optical depth is 4.8; and the standard deviation of cloud optical depth is 5.6. The first 15 of the cloud fields are shown in Figure 1. As expected for cumulus clouds, the LWC increases with height in the updraft cores, and the deeper clouds have larger LWCs.

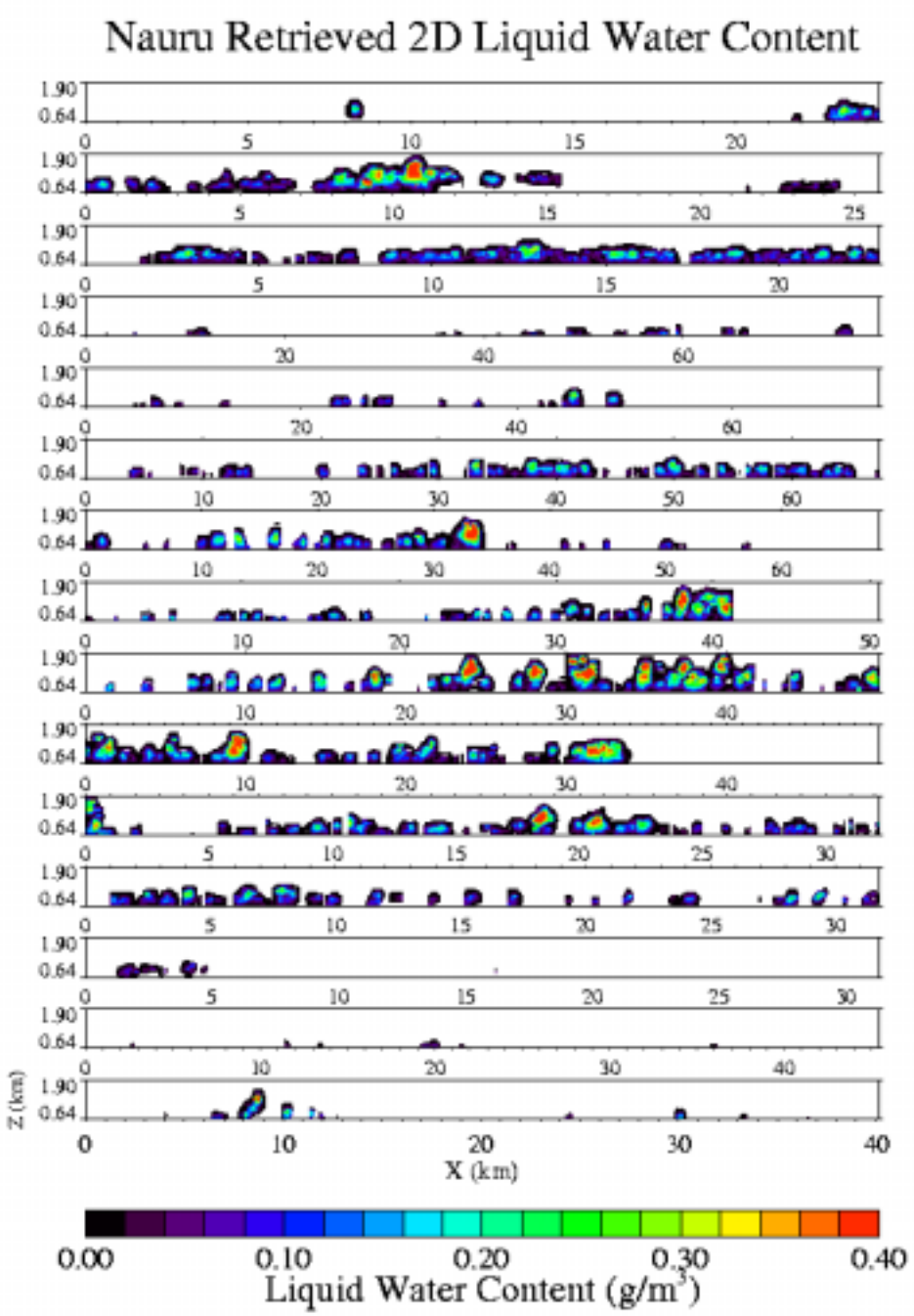

Figure 1. Radar-derived cloud LWC fields. Due to the different wind speeds, there is much variability in the size of the horizontal domain.

Stochastic Cloud Field Generation Method

A stochastic field generation algorithm can generate many random realizations of cloud fields using input statistics derived from data. If the two horizontal directions are assumed to be equivalent (horizontal isotropy), then 3D fields may be generated from statistics obtained from 2D radar-derived fields. We assume the statistics do not depend on horizontal location (translational invariance), but do depend on height. It is straightforward to produce fields having the correct single-point statistics (histogram or probability density function) for each vertical level. It is much more difficult to generate fields having the desired two-point and higher order statistics, which determine the spatial structure. One method for including two-point statistical information is Empirical Orthogonal Functions (EOFs). The advantage of EOFs is that the spatial structure of each EOF is determined solely by the data.

The basic algorithm for the stochastic field generation is to use independent gaussian noise of the appropriate variance for each EOF amplitude. The EOF amplitudes are by definition uncorrelated. Gaussian noise is used because the EOF transformation is linear, and the linear combination of gaussian random variables gives a gaussian distributed field. The correlated gaussian field is then transformed using the input cumulative distribution function (cdf) to produce the output extinction field having correct single-point statistics. Mathematically, let $e_l(x,z)$ be the l'th EOF, as a function of horizontal distance x and height z, with associated variance λ_l. Then a stochastic gaussian field g(x,z) is generated using random EOF amplitudes by

$$g(x,z) = \sum_{l=1}^{N} \sqrt{\lambda_l}\, Z_l e_l(x,z)$$

where Z_l are independent zero mean, unit variance gaussian random numbers. The gaussian field is transformed to the extinction field $\beta(x,z)$ using the cdf of extinction, $f(\beta;z)$, and the cdf of the standard normal distribution, n(Z):

$$\beta(x,z) = f^{-1}\left(n\left[g(x,z)\right];z\right)$$

where f^{-1} indicates the inverse function of the extinction cdf.

The use of EOFs for stochastic field generation is greatly facilitated by the fact that Fourier transforms are equivalent to EOFs for translationally invariant statistics. This is a result of the covariance matrix depending only on horizontal distance i-j and not on the two locations i and j; therefore $C_{ij} = C_{i-j}$, which is the autocorrelation function. Therefore, the eigenvalue equation defining the EOFs becomes a convolution equation

$$\sum_{J} C_{i-j} e_j = \lambda e_i$$

This convolution equation is solved in Fourier space where it becomes a simple multiplication by the Fourier transform of the autocorrelation function. In Fourier space the eigenvectors (EOFs) are delta

functions, and thus in real space the eigenvectors are sines and cosines. Hence, the Fast Fourier Transform (FFT) performs the EOF transformation.

The correlation function $\rho(z_1,z_2,r_{12})$ that defines the EOFs is a function of height of the two points z_1 and z_2 and the horizontal distance between the two points r_{12}. The difficulty here is that the correlation function is in the gaussian space, not the extinction space; hence, one cannot simply calculate the correlation function from the input extinction field. The obvious solution of transforming the extinction field to gaussian space using its cdf does not work because of the large fraction of zero extinction (clear pixels).

Since a gaussian field can be easily transformed to an extinction field, our approach instead is to find the gaussian space correlation that matches an extinction space two-point statistic. Adjusting the correlation gives only one degree of freedom, so the full two-point probability density function (pdf) cannot be matched. However, the binary (clear/cloud) two-point pdf can be matched exactly. While the binary two-point pdf has four probabilities ($P_{clear1,clear2}$, $P_{clear1,cloud2}$, etc.), it has only one degree of freedom beyond the single-point pdf. We take this approach because we believe that the cloud boundaries are the aspect of cloud structure most important for 3D radiative transfer. This correlation-matching procedure is performed for each pair of z levels and horizontal distance r bin (20 bins used here with log spacing out to approximately 512 pixels). A random sampling process computes the binary two-point extinction pdf from a range of gaussian correlations. Then the inverse process is performed to find the gaussian correlation that minimizes the difference between the measured and simulated binary two-point pdf.

The horizontal and vertical aspects of the stochastic field generation are partially separated. To generate the EOFs, first the autocorrelation function $\rho(r;z_i,z_j)$ at a large (e.g., 1024) number of evenly spaced positions x is cubic spline interpolated from the small (e.g. 20) number of distance bins. The EOF variances (eigenvalues) are found with an FFT in horizontal distance x of the autocorrelation function 3 for each pair of levels. This results in a small matrix $\rho_k(z_i,z_j)$ for each Fourier component k. A standard eigensolver routine is then used to compute the eigenvectors (EOFs) and eigenvalues (variances) of each matrix.

The transformation from EOF space to the gaussian real space is accomplished in two steps: 1) for each Fourier component k, the gaussian random EOF amplitude vector is multiplied by the $N_z \times N_z$ eigenvector matrix, and 2) for each z level a FFT over the k's is done. For 3D field generation, a 3D random EOF amplitude field is generated with variances depending the radial Fourier distance k, and a 2D FFT is done on each z level.

Since each element of the original correlation matrix is computed independently with a stochastic procedure, there is no guarantee that a valid, i.e., positive definite, correlation matrix results. Typically, there are some negative eigenvalues λ_l of the correlation matrix, but negative variances are not allowed. An optimization procedure is performed to adjust the elements of the square root matrix A to match the correlation matrix $\rho_k(z_i,z_j)$ within the error bars. Squaring A to get the correlation matrix assures that the eigenvalues are positive.

As is standard in EOF analysis, most of the EOFs are not used in the stochastic reconstruction. This is because many of the EOFs have low variances and are noisy due to the uncertainties in the correlation

matrix. An EOF is deleted if its eigenvalue is below an user specified absolute threshold or if its eigenvalue is below a specified fraction of the maximum eigenvalue for the particular Fourier component. There is some arbitrariness in picking the thresholds, but the generated fields are not overly sensitive to the choice.

A whole ensemble of stochastic fields are made at once. By forcing the ensemble of gaussian fields to have zero mean and unit variance, the correct single-point statistics (histogram) of the ensemble extinction fields is assured. This does not require that each extinction field have the same statistics, and indeed some have high cloud fraction while others are nearly clear. An outline of the stochastic cloud field algorithm is given below.

Statistics Collection Algorithm

Statistics collected: cdf of β for each level and gaussian correlations $\rho(z_1,z_2,r_{12})$.

1. Input an ensemble of 2D extinction fields $\beta(x,z)$ derived from radar.

2. Compute the cdf of discrete beta values for each level: $f(\beta; z)$.

3. Use random pixel sampling to compute two-point cloud/no cloud probabilities as a function of level z_1, level z_2, and horizontal distance r_{12}: $[P_{clear1,clear2}(z_1,z_2,r_{12}), P_{clear1,cloud2}(z_1,z_2,r_{12}), P_{cloud1,clear2}(z_1,z_2,r_{12}), P_{cloud2,cloud2}(z_1,z_2,r_{12})]$.

4. Use random sampling to find the gaussian correlation ρ that best matches each two-point probability set. This is done by transforming gaussian bivariate noise to extinction with the cdfs.

Stochastic Field Generation Algorithm

1. Fast Fourier Transform the correlation functions $\rho(r;z_i,z_j) \rightarrow \rho(k;z_i,z_j)$.

2. For each FFT component k use an optimization procedure to make the correlation matrix $\rho_k(z_i,z_j)$ positive definite.

3. Compute eigenvalues (EOF variances) and eigenvectors (EOFs) from the correlation matrices $\rho_k(z_i,z_j)$.

4. Delete EOFs with eigenvalues below absolute and relative thresholds.

5. Generate EOF amplitudes with gaussian noise (variance = eigenvalue).

6. FFT and matrix multiply to convert EOF amplitudes to gaussian fields g(x,y,z).

7. Force ensemble of gaussian fields to have zero mean, unit variance.

8. Use cdfs to convert to discrete $\beta(x,y,z)$.

The eigenvalue threshold were set so that 266 of the 28,672 EOFs were kept. Thirty 2D stochastic extinction fields of size 1024×28 were generated. These fields were then converted to cloud LWC and effective radius with the same lognormal droplet size distribution used in the radar retrieval. The second 15 of the 30 stochastic cloud LWC fields are shown in Figure 2. Visually the stochastic LWC fields do look similar to the radar-derived ones in Figure 1. Ten 3D stochastic extinction fields of size

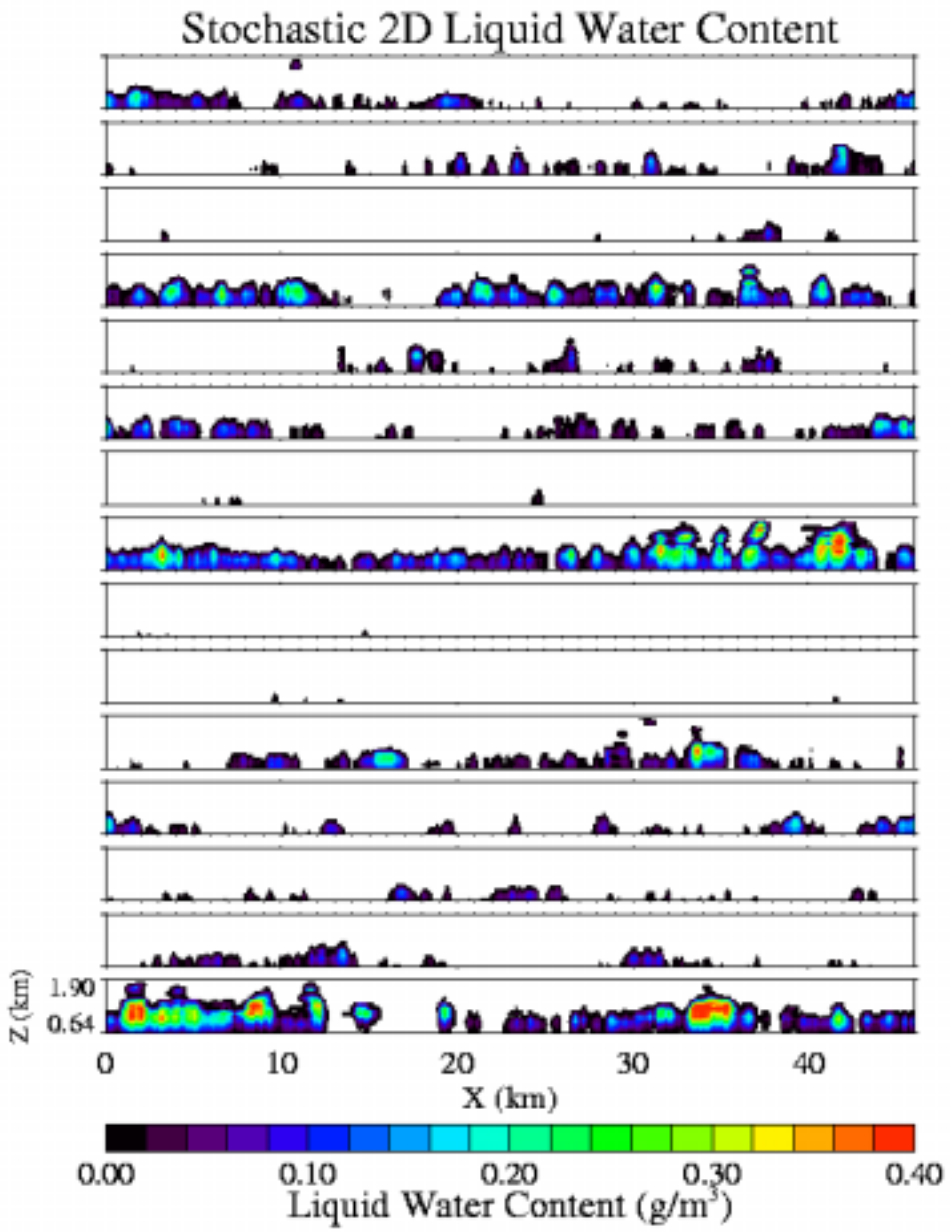

Figure 2. 15 of the 30 stochastically generated 2D cloud fields.

$512 \times 512 \times 28$ were produced. Figure 3 shows optical depth images for two of the 3D fields. For the ten 3D fields the cloud fraction is 37%; the mean cloud optical depth is 4.5; and the standard deviation of cloud optical depth is 6.1. These compare favorably with the optical depth statistics from the input radar derived fields, even though the optical depth distribution is not constrained to be reproduced exactly.

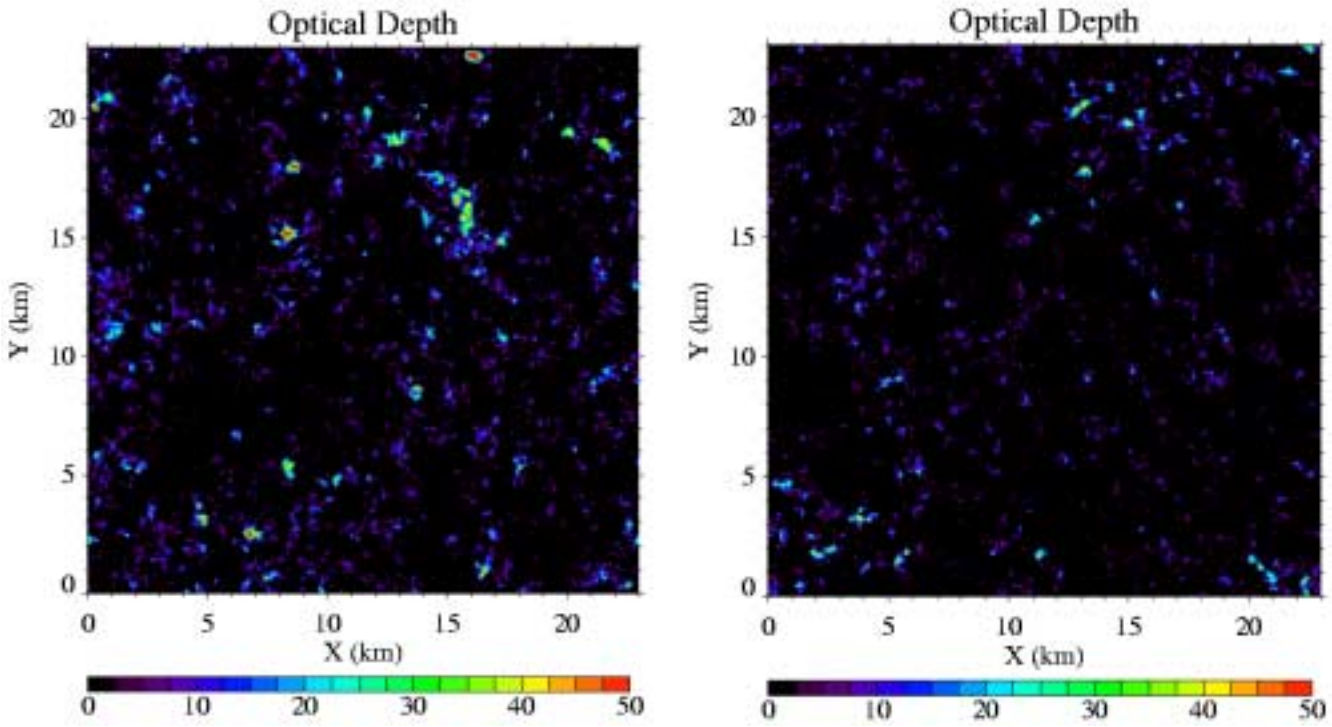

Figure 3. Optical depth images of two of the ten stochastically generated 3D cloud fields.

Radiative Transfer Modeling

Two broadband solar radiative transfer experiments are performed: 1) compare fluxes from the radar-derived and stochastic 2D fields to see if the stochastic fields are radiatively equivalent, and 2) compare fluxes from the stochastic 2D and 3D fields to determine how important the third dimension is for cumulus fields.

Broadband solar radiative transfer was calculated with a maximal cross section forward Monte Carlo code. Molecular absorption was included with the Fu and Liou (1992) 6-band correlated k-distribution. A mean atmospheric sounding for convectively suppressed conditions in the tropical west Pacific Ocean was input to the k-distribution. The cloud droplet optical properties were calculated with Mie theory for the LWC and effective radius fields obtained from the 75 droplets/cm^3 assumption. The Monte Carlo code calculates domain average fluxes for full 3D radiative transfer and the independent pixel approximation (IPA). Fluxes were calculated for five solar zenith angles (0, 27, 45, 56, 63) and a daytime average (overhead sun at noon). A 5% Lambertian surface albedo was assumed for all wavelengths. The number of photons spread across the 6 bands was 3×10^5 for each of the 30 2D

scenes and 1×10^6 for each of the 10 3D scenes. Because the purpose of the computation is a relative comparison, very high accuracy in the k-distribution and other radiative transfer assumptions is not important.

The mean reflected and total column absorbed fluxes over all the scenes are shown in Figure 4. The error bars indicate the standard deviation of the mean given the scene-to-scene variation. Having more scenes would reduce the errors. Figure 4a shows that there is good agreement in both reflected and absorbed fluxes between the radar derived and stochastic 2D cloud fields. This implies that the stochastic cloud fields are equivalent in terms of domain average radiative properties of the observed cloud fields.

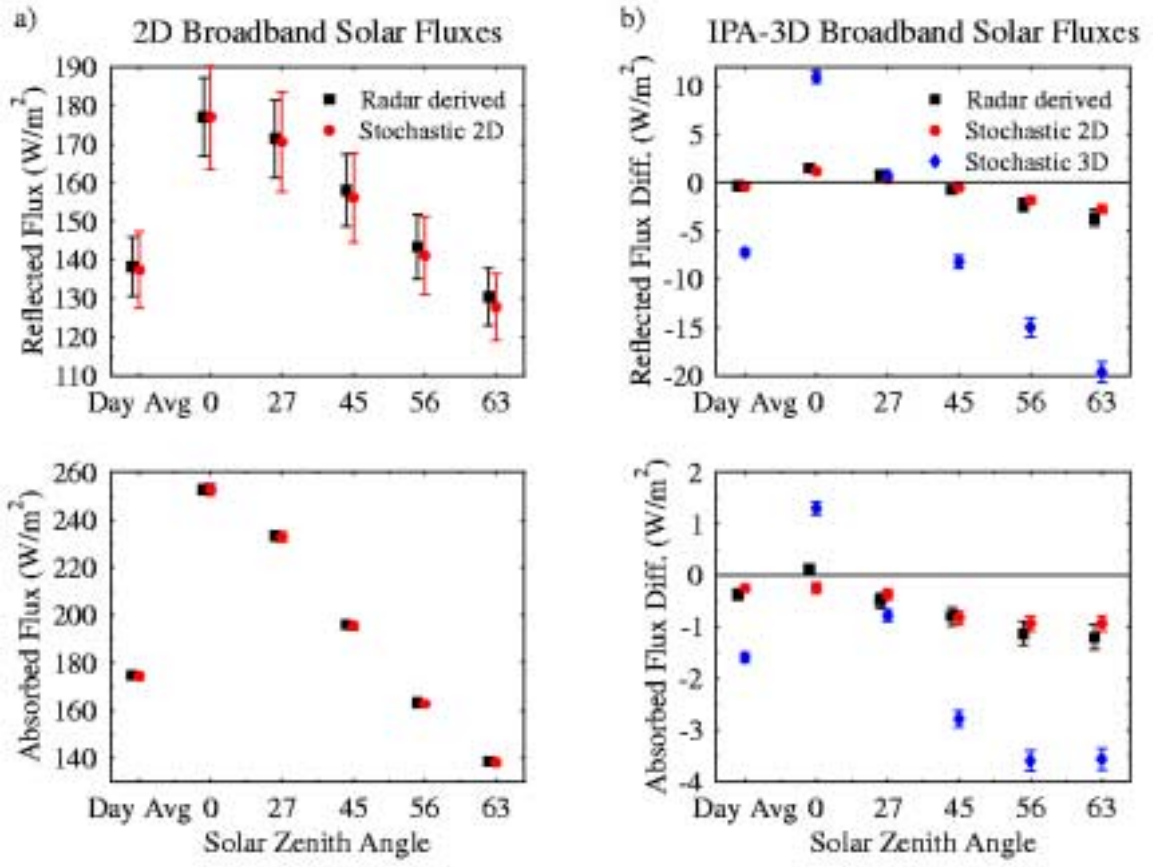

Figure 4. Broadband solar radiative transfer results. a) Reflected and absorbed flux for the 2D radar derived and 2D stochastic cloud fields. b) The difference between independent pixel approximation and 3D radiative transfer for the radar clouds and the 2D and 3D stochastic cloud fields.

The difference between the independent pixel approximation and 3D fluxes is a measure of the horizontal transport or 3D radiative effects of the clouds. Figure 4b shows the IPA-3D flux differences for the three types of cloud fields. The error bars are now much smaller due to the differencing. Again there is good agreement between the radar-derived and stochastic 2D cloud fields. However, the 3D cloud stochastic fields have a much larger 3D radiative effect than the 2D fields. This is presumably because the individual cumulus clouds in the 3D fields have much more side area over which the 3D

effects such as leakage can occur. The individual clouds in the 2D fields are actually streets with sides only in one dimension. As expected from the very similar optical depth statistics, the IPA fluxes agree well between the 2D and 3D stochastic fields (not shown).

Conclusions

A stochastic cloud field generation method based on EOFs was described. This method can create realistic random 3D cloud fields using statistics from 2D radar-derived cloud fields and assuming horizontal isotropy. The stochastic generation algorithm was applied to nonprecipitating cumulus clouds above Nauru in the tropical west Pacific Ocean. Broadband domain average solar radiative transfer calculations indicate that the 2D stochastic fields are radiatively equivalent to the original 2D radar-derived cloud fields. However, for these small cumulus clouds solar radiative transfer in 2D fields is not equivalent to transfer in 3D fields. The horizontal transport effects are much larger in the 3D stochastic fields due to their larger cloud side area.

These tropical cumulus cloud fields were selected to contain clouds, and so are not generally representative. In particular, the results on the importance of 3D radiative effects should not be considered to apply generally. The true cloud fraction of small tropical cumulus clouds is likely to be lower, and hence the size of the 3D effects would be reduced. To make these results more representative, many more cases are required. More robust cloud retrieval methods, including both MMCR radar and microwave radiometer data, should be used. Hourly winds from the 915-MHz profiler should be used instead of once-a-day radiosondes to advect the clouds. Hopefully, the diurnal cycle of cloud properties can be used to remove the Nauru island effect and make the results truly representative of tropical west Pacific oceanic cumulus clouds.

Acknowledgments

The authors thank Eugene Clothiaux for providing the preliminary Nauru ARSCL data. Financial support was provided by the Environmental Sciences Division of the U.S. Department of Energy (under grant DE-A1005-90ER61069 to the NASA Goddard Space Flight Center) as part of the ARM Program.

References

Barker, H. W., J.-J. Morcrette, and G. D. Alexander, 1998: Broadband solar fluxes and heating rates for atmospheres with 3D broken clouds. *Q. J. R. Meteorol. Soc*., **124**, 1245-1271.

Cahalan, R. F., W. Ridgeway, W. J. Wiscombe, T. L. Bell, and J. B. Snider, 1994: The albedo of fractal stratocumulus clouds. *J. Atmos. Sci*., **51**, 2434-2455.

Fu, Q., and K. N. Liou, 1992: On the correlated k-distribution method for radiative transfer in nonhomogeneous atmospheres. *J. Atmos. Sci*., **49**, 2139-2156.

Varnai, T., and R. Davies, 1999: Effects of cloud heterogeneities on shortwave radiation: Comparison of cloud top variability and internal heterogeneity. *J. Atmos. Sci*., **56**, 4206-4224.

Welch, R. M., and B.A. Wielicki, 1984: Stratocumulus cloud field reflected fluxes: The effect of cloud shape. *J. Atmos. Sci*., **21**, 3086-3103.